

COMPARISON OF TECHNOLOGY OF RADIATION VULCANIZED NATURAL RUBBER LATEX USING UV-MERCURY LAMP, UV-LED LAMP, AND PLASMA CATHODE-BASED EBM IRRADIATORS

Cahaya Widiyati^a, Herry Poernomo^{b*}

^aATK Polytechnic, Ministry of Industry, Campus-2, Jalan Prof. Dr. Wirdjono Prodjodikoro, Glugo, Panggunharjo, Sewon, Bantul, Yogyakarta 55188, Indonesia

^bResearch and Technology Center for Accelerator, Research Organization for Nuclear Energy, Jalan Babarsari Box Office 6101 ykbb Yogyakarta 55281, Indonesia

Article history

Received

22 August 2021

Received in revised form

16 February 2022

Accepted

28 February 2022

Published Online

20 April 2022

*Corresponding author
herr001@brin.go.id

Graphical abstract



Abstract

The electron beam machine (EBM) irradiators based on plasma cathode that emit pulse electron beam for radiation vulcanized natural rubber latex (RVNRL) have been developed in Tomsk, Russia. Meanwhile, a prototype of an ultraviolet light-emitting diode (UV-LED) irradiator for RVNRL has been developed by the Research Technology Center for Accelerator and the ATK Polytechnic in Yogyakarta, Indonesia. This research aims to compare the irradiator prototype technology for RVNRL. The RVNRL technology comparison method is carried out by assessing the specifications and performance of the equipment, costs (investment, operational, maintenance), hazard, and operability. The results of the comparison of irradiator technology for RVNRL show that the UV-LED irradiators are superior to the UV-mercury irradiators and the plasma cathode-based EBM irradiators which gives a total value of 476, 412, and 248, respectively. Thus, it can be concluded that the UV-LED irradiators technology for RVNRL is simpler, more practical, economical, and environmentally friendly compared to the UV-mercury irradiators and the plasma cathode-based EBM irradiators.

Keywords: RVNRL, irradiator, UV-mercury, UV-LED, plasma cathode-based EBM

© 2022 Penerbit UTM Press. All rights reserved

1.0 INTRODUCTION

The vulcanization of conventional natural rubber latex with the sulfur process requires 5 types of materials, which include antioxidants, sulfur binders for cross-linking polyisoprene, accelerators in the form of carbamate compounds, activating agents, and KOH stabilizers to prevent a pre-coagulation [1]. After the latex and 5 ingredients are mixed until they become homogeneous, it is heated at a temperature of 40-50 °C for 2-3 days. The second heating is at 70 °C for 2 hours, and the final heating is at 100 °C for 1 hour. The first and second heating is intended to make the vulcanization compound, while the final heating is the finishing stage.

Carbamate compounds must be compound the natural rubber latex to speed up the vulcanization process. The rubber product resulted is less elastic and produces a lot of SO_x gas, as well as it requires a storage time of approximately 3 weeks [1, 2].

Vulcanization at high temperatures can accelerate the time of vulcanization, thus lowering production costs. However, vulcanization at high temperatures causes uncontrolled side reactions resulting in lower product quality. While low temperatures to produce the quality, and appearance of natural rubber products are better than high temperatures, but it takes long vulcanization thereby increasing the cost of

production. The temperature of VNRL with sulfur process about 100-180 °C [3, 4]. Carbamate compounds can form carcinogenic compounds of nitrosamine in which the number of parts per billion (ppb) alone can cause cancer [5].

Cross-bonding produced by irradiated NRL vulcanization (RVNRL) is much stronger than that are produced by NRL vulcanization using sulfur. Because in the RVNRL cross-linking occurs directly between carbon atoms without going through sulfur atoms (C-C binding energy = 58.6 kcal/mol and C-S = 27.5 kcal/mol) as shown in Figure 1 [6].

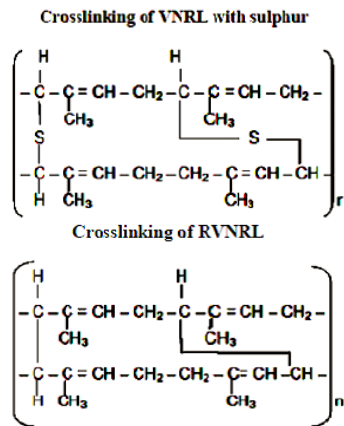


Figure 1 Crosslinking of VNRL with sulfur and RVNRL

1.1. The Advantage of UV Light Emitting Diode (UV-LEDs) Compared with UV-Mercury Lamp

The advantages of UVA rays from UV-LED compared to UVA/B rays of UV-mercury lamp is the wavelength spectrum of UVA rays than UV-LED has a wavelength of the electromagnetic (λ) at range about 360-380 nm narrower with UVA/B rays from UV-mercury lamp having a spectrum with a wide range of λ 240-420 nm as shown in Figure 2. The spectrum of UVA rays are narrow with $\lambda = 360-380$ nm of UV-LED lamps have a radiation sensitivity of 100% at a wavelength $\lambda = 375$ nm as shown in Figure 3 [7].

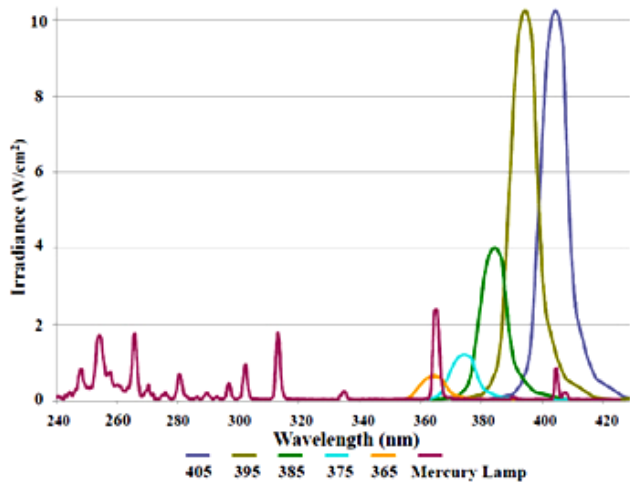


Figure 2 Spectrum irradiance of UV-LEDs radiation compared to UV rays than other lamps

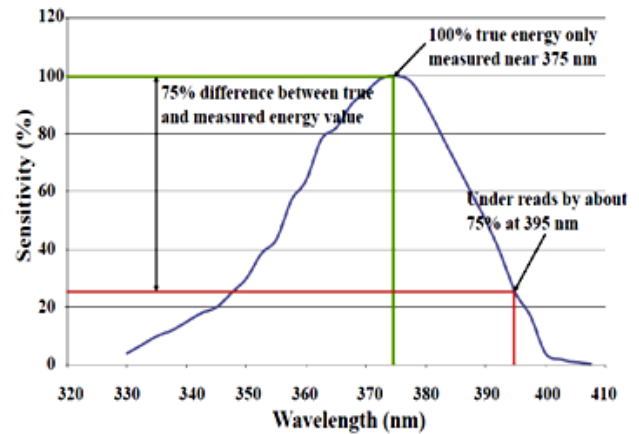


Figure 3 Type sensitivity of UVA rays

Figure 2 and Figure 3; shows that UV-A rays with a wavelength $\lambda = 375$ nm emitted by a UV-LED lamps are the best conditions if it is used in the curing process like to vulcanization NRL by irradiation.

Penetration of UVC rays with a wavelength $\lambda = 200-280$ nm in water reverse osmosis (RO) = 3.0 m; in drinking water = 12.0 cm; in (wine, juice) = 2.5 mm; in (syrup milk, blood) = 0.5 mm [8].

The ability of UVA rays penetrate larger than UVB rays and UVC rays, as shown in Figure 4 [9-11].

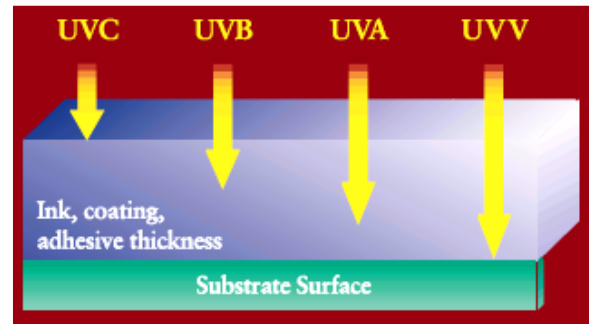


Figure 4 The ability to penetrate several types of UV rays

1.2. The Irradiator Prototype Based on UV-Mercury for RVNRL.

The research team from the Roseggerstraße Leoben Austrian Polymer Competence Center has succeeded in realizing the RVNRL pilot plant on the manufacture of non-allergenic surgical gloves using photoreactors with UVA/B rays radiation from UV-mercury lamps in the wavelength range of 240-420 nm. The form of a photoreactor is a vertical glass column with a diameter of about 13.5 cm and a length of about 1 m. In the middle of the glass column is hung UV-mercury lamps with specifications: power 3000 W, irradiance 1.1 W/cm², lamp length about 1 ft as a source of UVA/B rays radiation as shown in Figure 5 [12-15].

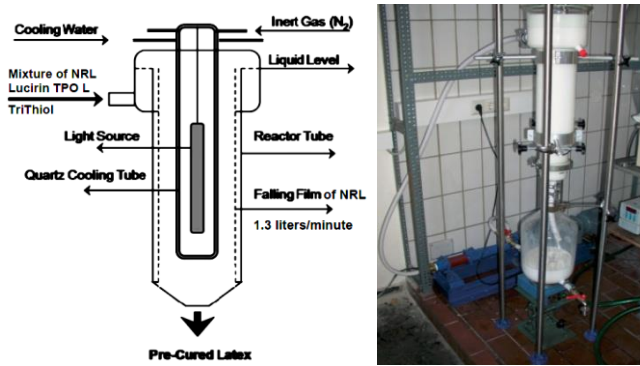
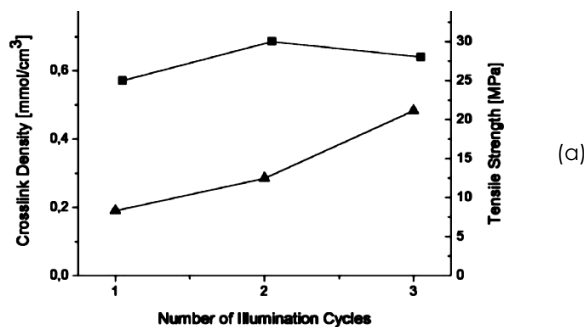


Figure 5 The irradiator prototype based on UV-mercury for RVNRL

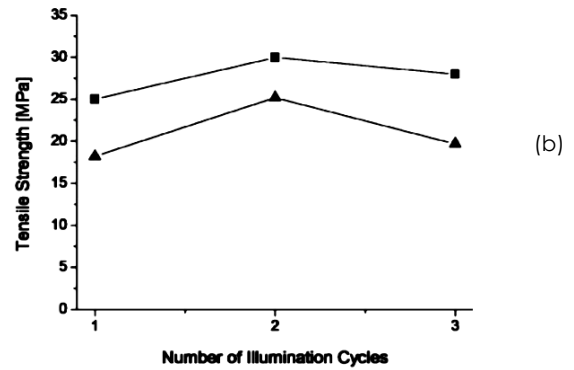
The RVNRL process is carried out by flowing a thin layer of NRL that has a density of 0.9162 g/cm^3 [16] by gravity at a flow rate of 1.3 liters/minute through the wall in the photoreactor. Twice illumination of UVA/B rays on a thin layer of NRL provides the results of mechanical tests on surgical gloves with a tensile strength of 30 MPa. However, with a single illumination of UVA/B rays on a thin layer of NRL, it can provide tensile strength to surgical gloves of 25 MPa which is above EN 455-2 (2000) standard with tensile strength before the 24 MPa aging process. The aging process of the pre-cured latex results from RVNRL at room temperature for 7 days showed mechanical tests on surgical gloves with a tensile strength of 23 MPa (for one-time illumination) and 28 MPa (for two times illumination) which were above EN 455-2 (2000) standard with a tensile strength of 18 MPa after the aging process [12].

The lifetime of UV-mercury lamps which emit UVA/B of about 500-2.250 hours [17-19], then for the continuity of the RVNRL process for a year would need several times of UV-mercury lamp replacement to be carried out so that it will inflict solid waste with mercury content that is classified as hazardous and toxic materials.

Mechanical tests of the surgical gloves from pre-cured latex resulted from RVNRL are expressed with tensile strength and crosslink density as shown in Figure 6 (a). Mechanical tests of surgical gloves from RVNRL pre-cured latex after aging at room temperature for 7 days are described with tensile strength as shown in Figure 6 (b) [12].



(■) Tensile strength in MPa and (▲) crosslink density in $\text{mmol}\cdot\text{cm}^{-3}$ of NR latex gloves pre-cured in the falling film reactor versus the number of illumination cycles



Tensile strength of non sterile NR latex gloves prior to and after thermal ageing (7 days / 70 °C / air) as a function of the number of illumination cycles in the falling film photoreactor: (■) Aged at room temperature for 7 days; (▲) Aged at 70 °C for 7 days

Figure 6 Characteristics of surgical gloves from pre-cured latex resulted from RVNRL

Figure 6 (a) shows that twice illumination provides the best mechanical test results for the surgical gloves from RVNRL pre-cured latex with 30 MPa tensile strength. However, even with one-time illumination, it turned out to have given a tensile strength in surgical gloves from RVNRL pre-cured latex at 25 MPa, which is above the standard EN 455-2 (2000) with a tensile strength of 24 MPa as shown in Table 1.

Figure 6 (b) shows that the aging process of RVNRL pre-cured latex at room temperature for 7 days shows the best mechanical gloves surgical test with the tensile strength of 23 MPa (for one-time illumination) and 28 MPa (for twice illumination), which are already above the standard EN 455-2 (2000) with 18 MPa tensile strength, as shown in Table 1 [12].

Table 1 Comparison of physical properties of sterile surgical gloves from RVNRL with UVA/B irradiation from UV-mercury lamps with the quality requirements of EN 455-2 (2000)

| Physical Properties | Sterile Surgical Gloves | | | |
|-------------------------|-------------------------|-------------|----------------------------|-------------|
| | EN 455-2 (2000) | | UV Pre-cured NR Latex Film | |
| | Before Aging | After Aging | Before Aging | After Aging |
| Tensile Strength (MPa) | 24 | 18 | 25–32 | 23–28 |
| Ultimate Elongation (%) | 750 | 560 | 770–870 | 680–720 |
| Force at Break (N) | 12 | 9 | 12.5–15 | 11.5–14 |

1.3. The Irradiator Prototype Based on UV-LED for RVNRL

Based on the characteristics of UVA rays from UV-LED irradiators which are superior to UVA/B rays from UV-

mercury irradiators, a prototype UV-LED irradiator for RVNRL in Center for Accelerator Science and Technology has been designed as shown in Figure 7 [20].



Figure 7 The irradiator prototype based on UV-LED for RVNRL

The novelty and advantages of the irradiator prototype based on UV-LED for RVNRL which was designed by Widiyati and Poernomo [20] is a technology development of a irradiator prototype based on UV-mercury designed by Schlögl *et al.* [12] are described as follows:

- The level of difficulty and the cost of construction work for the photoreactor prototype UV-LEDs is easier and cheaper when compared to photoreactor prototype UV-mercury in the vertical glass cylinder column.
- Replacement irradiators for the UV-LED are rarely needed because the lifespan of UV-LED lamps is around 50,000 hours while replacing the UV-mercury irradiators is done often the UV-mercury lamp's life span is only 2000 hours.
- Cost reduction in NRL molecular damage caused by NRL film temperature rise due to UVA/B heat radiation generated from UV-mercury irradiator as described in Figure 2 is relatively more expensive. This is because the cooling system used by N₂ gas injection is relatively expensive. The UVA radiation heat generated from the UV-LED irradiators such as Figure 3 is much smaller than UVA/B heat radiation from UV-mercury lamps. Thus, the cost of reducing the temperature rise in NRL films from UVA radiation is cheaper because the cooling system uses water only.
- Precision NRL film thickness on UV-mercury irradiators discharge is controlled by a piston pump and overflow NRL on a vertical glass cylinder. While the NRL film thickness on UV-LED irradiators more precision because it is controlled by a piston pump discharge, overflow NRL tank, and thick control indicator.

- The intensity of the radiation (irradiance) is influenced by the life of the UV-mercury lamp. Since the distance between UV-mercury irradiators with thin layer of NRL has been fixed, it is difficult to do on a prototype irradiance control UV-mercury irradiators. Meanwhile, if used UV-LED irradiators, it can be done by moving the irradiance control irradiator by a stepper motor on the instruction of irradiance indicator control.
- The process of installation/replacement of UV-LED irradiators and surface cleaning for vertical glass plate flow thin layer of NRL easier and faster when compared to the installation/replacement of UV-mercury irradiators and cleaning glass cylindrical column through which the thin layer NRL.

1.4. The Prototype of EBM Irradiators Based on Plasma Cathode for RVNRL

Another irradiator technology for the RVNRL process is electron beam machine (EBM) irradiators based on plasma cathode developed by Beam & Plasma Technologies LLC, Tomsk, Russia and the SB RAS Institute of High Current Electronics, Tomsk, Russia as shown in Figure 8 [21, 22]:



Figure 8 The prototype of EBM irradiators based on plasma cathode for RVNRL

The operating conditions and specifications of EBM irradiators based on plasma cathode in the RVNRL experiment are shown in Table 2 [21, 22].

Table 2 The operating conditions and specification of electron beam machine based on plasma cathode for RVNRL

| E-beam irradiation parameters | Value |
|---|-----------|
| Electron energy, E (keV) | 100 - 200 |
| Beam current, I (A) | up to 50 |
| Energy density/pulse, E_d (J/cm ²) | 0.06 |
| Pulse duration, P_d (μ s) | 5 - 35 |
| Total dose, D (kGy) | 183 |
| Beam repetition frequency, (Hz) | 0.1-50 |
| Main room, m ² | 6 x 6 |
| Operating room area, m ² | 2 x 2 |
| Room height, m | >4.5 |
| Width of ferroconcrete walls, m (for bio-shielding) | >1 |
| Number of pulses, N | 20,000 |
| Thick Al-Be foil, t_w (μ m) | 40 |
| Window size, $L \times s$ (mm) | 650 x 150 |
| Beam frequency, F (Hz) | 10 - 50 |
| Average beam power, kW | up to 5 |
| Supply voltage, V | 380 |
| Equipment power consumption, kW | up to 18 |
| Gas consumption N ₂ 99%, L/hour | 10 |
| Water consumption, m ³ /hour | 2 |

The configuration and size of EBM components based on plasma cathodes are shown in Figure 9 [22].

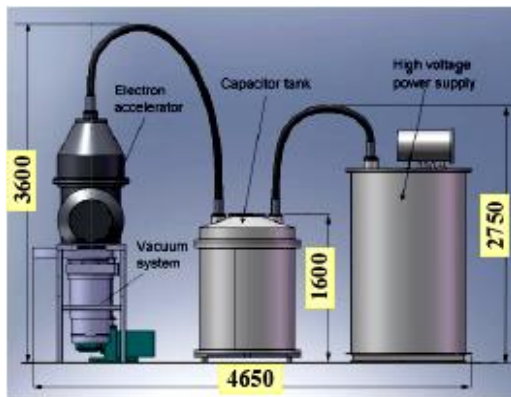


Figure 9 Size of components in the EBM irradiators based on plasma cathode for RVNRL

The N₂ gas consumption of 10 L/hr at EBM operations as shown in Table 1 is used to reduce the temperature rise in the foil window material due to bombardment by electron beams.

Based on the novelty and advantages of the irradiator prototype based on UV-LED compared to the irradiator prototype based on UV-mercury for the RVNRL process, the aim of this study was to compare the technology of two irradiators, namely the UV-LED irradiator which emits UVA radiation and the plasma cathode-based EBM irradiator which emits an electron beam for the RVNRL process. The results of the comparison of the irradiator prototype technology for the RVNRL process are expected to be input data for potential users to select and determine the type of irradiator suitable for use in the

NRL vulcanization process in several natural rubber plantation centers.

2.0 METHODOLOGY

2.1. Determination of RVNRL Capacity Using UVA/B Radiation from UV-Mercury Irradiators

Based on the flow rate data of the thin film NRL (Q) in the RVNRL pilot plant experiment by falling film photoreactor with UVA/B radiation from UV-mercury lamps [12], obtained:

Flow rate, $Q = (1.3 \text{ liters/minute}) = 1,300 \text{ cm}^3/\text{minute}$ (for 1 time illumination).

The highest usage of UVA/B lamps is only 3,000 hours (23). If the RVNRL process is operating 24 hours per day, then for the use of UVA/B lamps every 3,000 hours or 4.16 months would require a change. So that in the 1-year operation of the RVNRL process, UV-A lamps must be replaced 3 times. If the prediction of each UV-mercury lamp replacement requires around 2 days of unloading, then the remaining number of days in an RVNRL operating year = 324 days.

Mechanical tests of the surgical gloves pre-cured NRL resulted from RVNRL in Figure 4 shows that the tensile strength and the crosslink density is best achieved at twice the illumination of the film NRL. If the discharge NRL film that flows in the annulus glass photoreactor is at $1,300 \text{ cm}^3/\text{min}$, the capacity of RVNRL (M) can be calculated as follows (20):

$$M = \text{flow rate (cm}^3/\text{min)} \times \text{NRL density (g/cm}^3) \quad (1)$$

2.2. Determination of RVNRL Capacity Using UVA Radiation from UV-LED Irradiators

Based on data from debit of NRL film (Q) in the experimental pilot plant VNRLI are falling film irradiators with radiation UV-A/B of UV-mercury lamp, it can be determined linear flow rates thin layer of NRL (v) for vulcanization NRL with the best results as follows [23]:

$$v = Q / (\pi \times ID \times t_b) \quad (2)$$

with v = flow rate of NRL (cm³/min), ID = inside diameter of the column (cm), t_b = thickness penetration of UV-A (cm)

Calculation capacity of VNRLI using irradiators of UV-LED lamps needed about 6 UV-LED lamp T8 TL shape with a length of 2 feet, the intensity of the radiation (irradiance) $I \geq 1.1 \text{ W/cm}^2$ mounted horizontally lined up shoulder to shoulder with the following calculation [23]:

$$Q = v \times t_b \times L \quad (3)$$

with v = flow rate of NRL (cm³/min), t_b = thickness penetration of UV-A (cm), L = width of vertical glass plate flow-thin layer NR.

2.3. Determination of RVNRL Capacity Using Electron Beam Radiation from EBM Prototypes Based on Plasma Cathode

Test of the EBM prototype based on plasma cathode for the RVNRL process was carried out as shown in Figure 10. The distance of the payer window to the conveyor surface is a maximum of 30 mm. NRL feed is channeled to the conveyor at a certain flows speed so that a thin layer of NRL can form on the conveyor. Then the thin layer on the conveyor that runs at a certain speed was irradiated with an electron beam. The thin layer of irradiated NRL is sliced with a knife, then contained in a container as shown in Figure 10 [22].

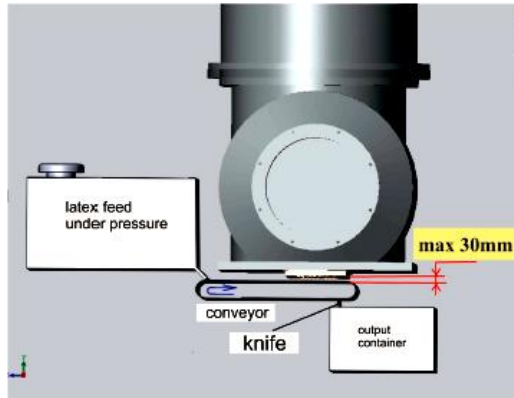


Figure 10 Test of the EBM prototype based on plasma cathode for the RVNRL process

For the pulse beam electron system, the absorbed dose (D) in units of kGy or J/kg in a material with mass m (grams) is determined as follows [24]:

$$D = \frac{E}{m} = \frac{U \times j \times t_{beam} \times N}{\rho \times h} \quad (4)$$

where, E = electron beam energy deposited into the material (volt.amp.sec, watt.sec or J), U = accelerator voltage (volts), j = beam current density (amp/cm²), t_{beam} = duration of beam pulses electron (second), N = number of beam pulses, ρ = material density (g/cm³), h = depth of electron beam penetration in the irradiated material (cm).

Multiplication U (volts) \times j (amperes/cm²) \times t_{beam} (seconds) in units of volts. amperes/cm² \times seconds or watts \times seconds/cm² or (J/cm²) is a unit of energy density per pulse (Ed) of EBM prototype based on plasma cathode as listed in Table 1.

Thus the electron beam energy deposited into a material (E) from Equation (5) is analogous to the total energy density (Ed_T) of the EBM prototype based on plasma cathode-base as stated as follows [2]:

$$Ed_T = Ed \times N \quad (5)$$

where, Ed = energy density per pulse (J/cm²), N = number of pulses.

Whereas ρ (g/cm³) \times h (cm) the result has a unit (g/cm²) which is analogous to the electron beam penetration unit, R or Pt (g/cm²).

D absorbcency dose is calculated as follows [2]:

$$D = E \times j_{a \times t} \times 10^6 / R \quad (6)$$

The absorbed dose D of the electron beam in Equation (3) is analogous to D in Equation (4) of the electron beam. Thus, D in the Equation (4) can be converted as follows [2]:

$$D = \frac{Ed_T}{P_t} \quad (7)$$

Thus, the electron beam penetration before passing through the window is calculated as follows [2]:

$$P_t = Ed_T / D \quad (8)$$

where, P_t = electron beam penetration (g/cm²), D = absorbed dose (kGy or J/kg or W \square sec/kg).

The EBM prototype was based on plasma cathodes with electron beam pulses at a certain duration (Pd) and frequency (F), then the total power can be calculated as follows:

$$P_e = E \times I \times Pd \times F \quad (9)$$

where, P_e = required power (watts), E = electron beam energy (volts), I = electron beam current (ampere), Pd or t_{beam} = pulse duration (second), F = frequency (Hz or cps or cycles/second).

The maximum NRL thin layer that can be penetrated by the electron beam (t_b) can be calculated as follows [2]:

$$t_b = \frac{0.9 \times P_t - [(t_w \times \rho_w) + (t_u \times \rho_u)]}{\rho_b} \quad (10)$$

where, P_t = electron beam penetration (g/cm²), t_w = foil window thickness (cm), ρ_w = foil window density (g/cm³), t_u = air gap thickness (cm), ρ_u = air density (g/cm³).

Correlation of linear velocity v (m/sec) NRL thin layer irradiated with electron deposition energy per area density De (MeV cm²/g), electron beam current I (mA), efficiency factor (η), absorbcency dose D (kGy or kJ/kg or kW.second/kg), window width s (m) is expressed as follows [25]:

$$D = (De \times \eta \times I) / (10 \times s \times v) \quad (11)$$

$$v = (De \times \eta \times I) / (10 \times D \times s) \quad (12)$$

De can be determined as follows [25]:

$$De = E/z = P_e / (z \times I) \quad (13)$$

Thus Equation (12) changes as follows::

$$v = (P_e \times \eta \times I) / (10 \times z \times D \times s \times I) \quad (14)$$

$$v = (P_e \times \eta) / (10 \times z \times D \times s) \quad (15)$$

$P_e = E \times I$ with, P_e = power (watt.seconds or J), E = electron beam energy (MeV), I = electron beam

current (mA), z or P_t' = penetration of electron beams on material (g/cm^2), t = time (seconds).

By adopting the v belt conveyor determination in Equation (15), it can be determined the linear flow velocity of the NRL thin film above the conveyor belt v (m/sec) with the electron beam from the cathode-based EBM plasma as shown in Figure 10.

Operating variables of EBM based on plasma cathode include electron beam energy E (MeV), electron beam current I (mA), efficiency factor (η), P_d pulse duration, frequency F (Hz or cps), absorbed dose D (kGy or kJ/kg or kW.sec/kg), window width s (m).

Thus, by substituting Equation (9) turns into Equation (15) can be obtained as follows:

$$v = (E \times I \times P_d \times F \times \eta) / (10 \times P_t' \times D \times s) \quad (16)$$

The flow rate of the NRL film above the irradiated belt conveyor can be determined as follows [2]:

$$Q = v \times A \quad (17)$$

with, Q = flow rate in the NRL films on belt conveyor (cm^3/sec), A = area of NRL film with the thickness as the electron beam penetration (cm^2). Consequently, the rate of latex film corresponding to the electron beam penetration can be calculated as follows [2, 23]:

$$Q = v \times (t_b \times L_w) \quad (18)$$

where, L_w = window length (cm).

Capacity of RVNRL (M , g/sec) can be calculated as follows [20]:

$$M = Q \times \rho_b \quad (19)$$

2.4. Efficiency for Electron Beam Accelerators

The electrical energy conversion efficiency for electron beam accelerators, the ratio of the input electrical power to output beam power, ranges between 25% to 75% depending upon the design of a specific accelerator [26].

Pulse-based electron beam machine with high frequency (HF) accelerator and technical specifications: energy about 1-10 MeV, pulse duration of 1 ms^{-1} , beam power about 30-50 kW, beam current about 0.1-1 A provides an efficiency of 30% [27].

When EBM is operated, the electron beam that passes through a material, such as windows and air gaps, the energy, and power of the beam will be reduced by the events of backscattered electrons and adsorption by the material.

The greater the initial electron beam energy in the use of EBM, the smaller the energy loss and beam power as shown in Table 3 [28]:

Table 3 Energy and beam power losses in double foil window construction (two 50 μm thick titanium foils and 70 mm air gap between them) for 50 kW average beam power and initial electron energy 0.5, 0.6, 0.7 MeV

| Initial electron energy, keV | 500 | 600 | 700 |
|--|------|------|------|
| Windows | | | |
| - backscattering, % | 24.9 | 17.8 | 12.2 |
| - absorption, % | 13.5 | 11.9 | 9.3 |
| Air gap | | | |
| - absorption, % | 2.5 | 2.0 | 1.7 |
| Total of energy and beam power losses, % | 40.9 | 30.8 | 23.2 |

3.0 RESULTS AND DISCUSSION

3.1. The RVNRL Capacity Using UVA/B Radiation from UV-Mercury Irradiators

The RVNRL experiment with UV-mercury irradiator showed that the best irradiated NRL was at 2 times NRL illumination, so M had to be multiplied by 0.5.

From the results of the RVNRL capacity calculation using UV-mercury irradiators, then from Equation (1) can be obtained as follows:

$$M = 1,300 \text{ cm}^3/\text{min} \times 0.913 \text{ g}/\text{cm}^3 \times 0.5 = 593.45 \text{ g}/\text{min}.$$

$$M = 593.45 \text{ g}/\text{min} \times 60 \text{ minutes}/\text{hour} \times 24 \text{ hours}/\text{day} \times 324 \text{ days}/\text{year}.$$

$$M = 276 \ 880 \ 032 \text{ g}/\text{year} = 276.88 \text{ tons}/\text{year}.$$

If it is assumed in the film isoprene, irradiated isoprene NRL (i-isoprene) caused by radiation crosslinking of isoprene by UVA/B with a conversion of about 90%, then:

$$M = 0.90 \times 276.88 \text{ tons}/\text{year} = 249.2 \text{ tons}/\text{year}.$$

The quality of RVNRL results using UVA/B radiation from a UV-mercury lamp is represented by a tensile strength of 28 MPa as shown in Figure 6.

3.2. The RVNRL Capacity Using UVA Radiation from UV-LED Irradiators

From Equation (2), it can be calculated as follows:

$$v = (1,300 \text{ cm}^3/\text{min}) / [(\pi \times 13.5 \text{ cm})(0.05 \text{ cm})] = 612.794 \text{ cm}/\text{min}.$$

Figure 2 shows that the wavelength range of UV-mercury lamps are very wide = 240-420 nm with varying irradiance. If used UV-LED light with a wavelength of about 365-375 nm, the obtained irradiance that is more focused about $1.1 \text{ W}/\text{cm}^2$.

Figure 3 shows that the wavelengths of 375 nm in the UV-A rays arising from UV-LED lamps have a sensitivity of 100%. Thus UV-A radiation from the UV-LED lamps have a greater ability to curing (cross-linking) poly-isoprene in the NRL compared with UV-A/B from UV-mercury lamps.

Capacity of RVNRL can be increased by increasing the bandwidth trajectory thin layer of NRL that will be irradiated with UV-A rays of UV-LED

irradiators and debit-based on flow rate of NRL thin layer, $Q = 1.3$ liters/minute to process irradiators RVNRL with UV-mercury lamps which have been performed by S.Schlögl, *et al.* in the Polymer Competence Center Leoben, Austria as shown in Figure 5 [12].

Calculation capacity of RVNRL using irradiators of UV-LED lamps needed of 6 UV-LED lamp T8 TL shape with a length about of 2 feet, the intensity of the radiation (irradiance) $I \geq 1.1$ W/cm² mounted horizontally lined up shoulder to shoulder with calculation using Equation (3) with $L =$ width of vertical glass plate flow-thin layer NRL of 40 cm.

$$Q = 612.794 \text{ cm}^3/\text{min} \times 0.05 \text{ cm} \times 40 \text{ cm} = 1,225.6 \text{ cm}^3/\text{min} = 1.225 \text{ L}/\text{min}.$$

By using Equation (1) the RVNRL capacity (M) can be calculated as follows:

$$M = 1,225.6 \text{ cm}^3/\text{min} \times 0.913 \text{ g}/\text{cm}^3 = 1,118.97 \text{ g}/\text{min}.$$

$$M = 1,118.97 \text{ g}/\text{min} \times 60 \text{ min}/\text{hour} \times 24 \text{ hours}/\text{day} \times 330 \text{ days}/\text{year}.$$

$$M = 580,075,499.52 \text{ grams}/\text{year} = 580 \text{ tons}/\text{year}.$$

If the assumed conversion of poly-isoprene in the film NRL by UV-A rays of irradiators UV-LED into poly-isoprene irradiated (i-polyisoprene) caused by crosslinking chain C in poly-isoprene with free radicals thyl formed as photoinitiator thiolene irradiated UV-A is about 90%, then:

$$\text{Capacity of RVNRL} = 0.90 \times 580 \text{ tons}/\text{year} = 522 \text{ tons}/\text{year}.$$

If it is seen from the penetration of UVA radiation that is greater than the penetration of UVB rays on the material as shown in Figure 4, then the penetration of UVA radiation from the UV-LED lamp will be greater than the penetration of UVA/B rays from the UV-mercury lamp on the material. Because the penetration of UVA emitted from UV-LED lamps is greater than the penetration of UVA/B from UV-mercury lamps, it is predicted that the cross-linking process of poly-isoprene on natural rubber latex irradiated with single UVA rays emitted from UV-LED lamps will be more. Thus it can be predicted that the quality of RVNRL results using UVA radiation from UV-LED lamps represented by tensile strength will be greater about 30 MPa than the tensile strength of RVNRL results using UV-mercury lamps of 28 MPa as shown in Figure 6.

3.3. Penetration of Electron Beams (P_t) on Changes in Electron Beam Energy (E)

To determine the depth of the electron beam penetration in the NRL film, the dose distribution of the electron beam penetration is needed in general. Curve of relative dose distribution ($D_{relative}$) vs electron beam penetration (R or P_t) can be drawn as shown in the Figure 11, with $D_{(z)}/D_{max} = D_{relative}$.

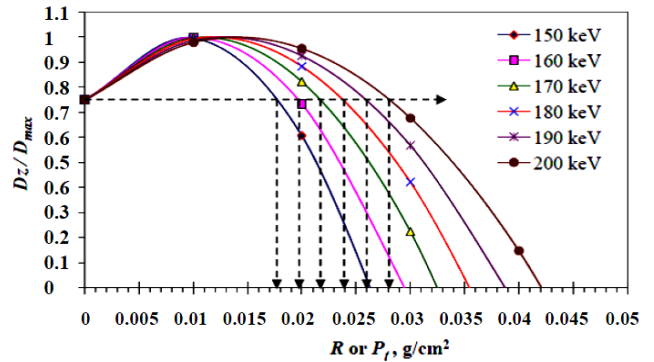


Figure 11 D_z/D_{max} vs P_t on e-beam energy variations.

At D_z/D_{max} or $D_{relative} = 0.75$ a straight line is drawn across the curve at 150 keV, 160 keV, 170 keV, 180 keV, 190 keV, and 200 keV, then from the intersection point a straight line is drawn which intersects the abscissa of R or P_t respectively at $P_t = 0.0178; 0.0198; 0.0215; 0.0238; 0.0258; 0.0280$ g/cm².

3.4. The Efficiency of Energy and Beam Power on the EBM Based on Plasma Cathode

Based on the data in Table 3, the relationship curve between initial energy with energy and beam power losses on the EBM operation is obtained as shown in Figure 12.

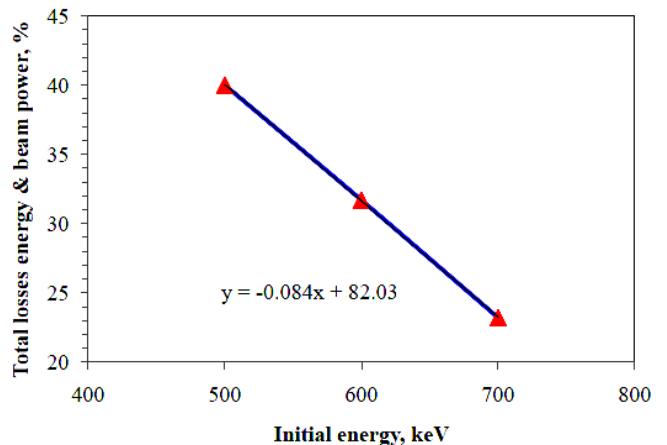


Figure 12 The effect of initial energy on the energy and beam power losses total

The graph of the initial energy effect on energy loss and beam power as shown in Figure 12 can be expressed as follows (20):

$$y = -0.084x + 82.03 \tag{20}$$

where, $y =$ total energy and beam power losses (%), and $x =$ initial energy (keV).

From Equation (20), we can calculate the effect of initial energy EBM 150 keV, 160 keV, 170 keV, 180 keV, 190 keV, and 200 keV on the total energy and beam power losses, and the residual energy and beam power as shown in Table 4.

Table 4 Energy and beam power losses in foil window construction (40 μm thick Al-Be foils and 30 mm air gap between them) for 5 kW average beam power and initial energy 150, 160, 170, 180, 190 keV

| Initial electron energy, keV | 150 | 160 | 170 | 180 | 190 | 200 |
|--|-------|-------|-------|-------|-------|-------|
| Total of energy and beam power losses, % | 69.28 | 68.59 | 67.75 | 66.91 | 66.07 | 65.23 |
| The residual of energy and beam power, keV | 46.08 | 50.25 | 54.82 | 59.56 | 64.47 | 69.54 |
| The efficiency of energy and beam power, % | 30.72 | 31.40 | 32.24 | 33.09 | 33.93 | 34.77 |

The energy efficiency and electron beam power obtained in Table 3 are within the range of electron beam power efficiency of 0.2 - 0.7 as stated by Zimek [26], as stated in International Irradiation Association [27] with the efficiency of 25% to 75%, and almost equal to 30% efficiency as stated by Zimek [28].

3.5. RVNRL Capacity Using Electron Beam Radiation from the Plasma Cathode-Based EBM Irradiators

The operating conditions of the plasma cathode-based EBM irradiators that can be adjusted are the pulse electron beam energy ($E = 100\text{-}200$ keV) and the strong current ($I =$ up to 50 A) as shown in Table 2. The efficiency of the EBM tool (η) depends on the performance of each equipment such as HV power supply, battery capacitor, electron accelerator, and vacuum system as shown in Figure 8.

According to Patent 7026749 [29], the lifetime of the cathode is 20,000 - 25,000 hours. If the cathode material used by the plasma cathode-based EBM irradiators it is assumed to be the same as the cathode material used in Patent 7026749, then in an operational year for RVNRL no cathode replacement is needed. Thus, in one year the RVNRL process is the number of effective days = 330 days.

By using data of $\rho_{latex} = 0.9162$ g/cm³ [16], $\rho_w = 2.1$ g/cm³ [30], $\rho_v = 0.00112$ g/cm³ [31], $t_w = 3$ cm [22], and some process condition data and EBM-based plasma cathode specifications in Table 2 consisting of: $t_w = 40$ μm, $F = 50$ Hz, $D = 183$ kGy, $Ed = 0.06$ J/cm², $Pd = 35$ μs, $N = 20,000$ pulses, η from Table 4 = 34.77%, then from the empirical Eqs. (16), (18) and (19) can be obtained RVNRL capacity (M) as in Table 5:

Table 5 The effects of E and I on RVNRL capacity (M)

| E (keV) on $I =$ | M | I (Ampere) on | M |
|--------------------|-------------|-----------------|-------------|
| 26 A | (tons/year) | $E = 200$ keV | (tons/year) |
| 150 | 99.83 | 14 | 95.19 |
| 160 | 116.32 | 16 | 108.79 |
| 170 | 131.20 | 18 | 122.39 |
| 180 | 146.80 | 26 | 176.79 |
| 190 | 161.64 | 40 | 271.98 |
| 200 | 176.79 | 50 | 339.98 |

The results of empirical calculations of the capacity of RVNRL in the operating conditions of the plasma cathode-based EBM irradiators: $E = 200$ keV, $I = 26$ A, $F = 50$ Hz, $D = 183$ kGy, $Ed = 0.06$ J/cm², $Pd = 35$ μs, $N = 20,000$ pulses, and the efficiency of the tool $\eta = 34.77\%$ obtained RVNRL capacity as follows: $M = 176.79$ tons/year.

An experiment of a plasma cathode-based EBM irradiator has been carried out for the RVNRL process at a maximum energy condition of 200 keV and $I = 26$ A at Beam & Plasma Technologies LLC, Tomsk, Russia. The experimental results showed that the tensile strength of the NRL product after irradiation was 21 MPa, and the RVNRL capacity was 0.5 tons/day [22].

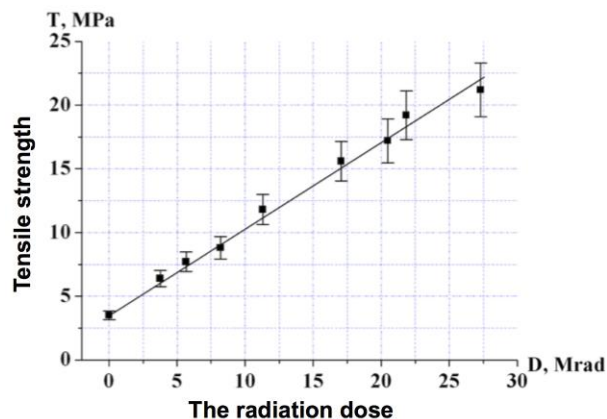
If in one year the RVNRL operation is carried out for 330 days, then the RVNRL capacity from the results of the plasma cathode-based EBM irradiator experiment is as follows:

$$M = 0.5 \text{ tons/day} \times 330 \text{ days/year} = 165 \text{ tons/year.}$$

The results of the empirical calculation of the RVNRL capacity and the real data of RVNRL capacity from the experimental results of the plasma cathode-based EBM irradiator at conditions of $E = 200$ keV and $I = 26$ A gave results of $M = 176$ tons/year and 165 tons/year, respectively. Because M results from empirical calculations and from experimental results are almost the same, then the empirical Equation. (4) to (19) can then be used as an initial step to determine the capacity of the RVNRL which applies specifically to plasma cathode-based EBM irradiators.

If the calculation of RVNRL capacity uses the empirical Eqs. (16), (18) and (19) on EBM based on plasma cathodes at maximum operating conditions: $E = 200$ keV with $\eta = 34.77\%$, $I = 50$ A, $Pd = 35$ μs, $D = 183$ kGy/kg, $F = 50$ Hz, $N = 20,000$ pulses, $Ed = 0.06$ J/cm²; then it can be obtained $M = 339.98$ tons/year.

The performance of plasma-based EMB for the RVNRL process under conditions of electron beam energy $E = 200$ keV and electron beam current $I = 26$ A obtained the characteristics of irradiated latex as shown in Figure 13.



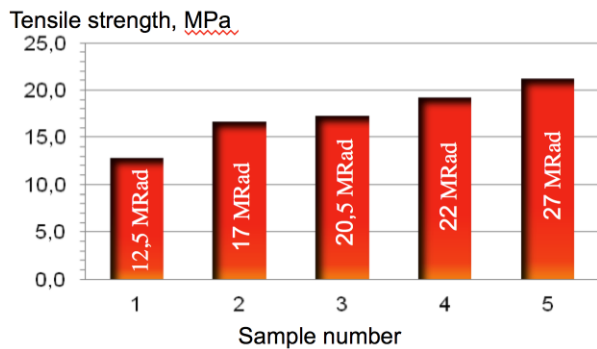


Figure 13 Characteristics of latex irradiated by pulsed electron beam from plasma-based EMB

The tensile strength of latex irradiated with pulsed electron beams from plasma-based EBM in Figure 13 when compared with the results of latex irradiated with ultraviolet light from a UV-mercury irradiator in Figure 6 and Table 1, it shows that the tensile strength of latex irradiated with ultraviolet light greater than the tensile strength of latex irradiated with a pulsed electron beam from plasma-based EBM. This indicates that the quality of the latex irradiated with ultra violet light is better than the quality of the latex irradiated with a pulsed electron beam from plasma-based EBM.

RVNRL research using EBM based on a continuous electron beam from an electron gun with tungsten filament material has been carried out by Hani Handayani *et al.* (2019) at an electron energy of 300 keV and a current of 3 mA. The RVNRL process was carried out at doses of 50, 70, 90, 110, 130, and 150 kGy resulting in the tensile strength quality of irradiated latex 0.2; 0.9; 0.4; 0.1; 0.4; 0.4 MPa or N/mm² [32].

RVNRL research using the same EBM at an electron energy of 300 keV and a current of 3 mA has also been carried out by Elin Nuraini *et al.* (2021) with a latex film thickness of 0.4 mm produced a tensile strength quality of irradiated latex of 5.61 N/mm² [33].

RVNRL research using EBM based on a continuous electron beam from an electron gun at an electron energy of 8 MeV at a radiation dose of 150, 200, 250

kGy has also been carried out by Manuchet Reowdecha *et al.* (2021) with tensile strength quality of irradiated latex 12.2 and 15.8 MPa, respectively [34].

The use of electron beam-based EBM for three RVNRL researches as has been done by Hani Handayani *et al.* (2019), Elin Nuraini *et al.* (2021), and Manuchet Reowdecha *et al.* (2021) have not met the quality of latex for the manufacture of post-aging surgical gloves as required by EN 455-2 (2000) for medical examination gloves with a tensile strength of 18 MPa as shown in Table 1 [12].

The irradiated latex from plasma cathode-based EBM at a radiation dose of 270 kGy as shown in Figure 13 had better tensile strength qualities when compared with the tensile strength of irradiated latex from the RVNRL process of 3 continuous electron beam-based EBM.

3.6. Comparison of Irradiator Prototype Technology for RVNRL

Comparison of irradiator prototype technology for RVNRL using pulse electron beam radiation from the plasma cathode-based EBM irradiators and UVA radiation from UV-LED lamp irradiators is done by scoring (S) on the two types of irradiators. Scoring of irradiator characteristics is classified into 3 groups, namely group A: tool performance, group B: costs (investment, operational, and maintenance), group C: hazardous and operability (HAZOP).

Each irradiator characteristic has a level (L) of 1-4 with a distribution: 4 = very important, 3 = important, 2 = quite important, 2 = not important. Each level has a value (V) of 1-10 with each level a different characteristic irradiator.

The value of each irradiator's performance (S) can be approximated as follows [35]:

$$S = V \times L \tag{21}$$

The results of the comparison of EBM irradiator prototype technology based on plasma cathodes and UV-LED irradiator prototype technology for the RVNRL process are shown in Table 6, 7, 8 and 9.

Table 6 Comparison of irradiator prototype technology for RVNRL in terms of quality of the RVNRL products and equipment performance

| Type of irradiator | Tensile strength of the RVNRL products (MPa) | | The RVNRL capacity (tons/year) | | Start-up of irradiator (hours) | | Life time irradiator (hours) | | ΣS |
|--------------------|--|----|--------------------------------|----|--|----|------------------------------|----|------------|
| | L = 4 | S | L = 4 | S | L = 4 | S | L = 4 | S | |
| EBM Plasma Cathode | 21.25, V = 3 | 12 | 165, V = 3 | 12 | Vacuum system = 2 (Slow), V = 5 | 20 | 25,000 (Medium), V = 5 | 20 | 64 |
| UV-Mercury | 28, V = 5 | 20 | 249.2, V = 5 | 20 | 5–10 seconds (Very fast), V = 10 | 40 | 3,000 (Short), V = 3 | 12 | 92 |
| UV-LED | 30, V = 7 | 28 | 522, V = 8 | 32 | 5–10 seconds (Very fast), V = 10 | 40 | 50,000 (Long), V = 10 | 40 | 140 |

Table 7 Comparison of irradiator prototype technology for RVNRL in terms of investment costs

| Type of irradiator | Prediction of irradiator and supporting equipment costs | | Prediction of radiation shield costs | | Prediction of irradiator construction & installation costs | | ΣS |
|--------------------|---|----|---|----|--|----|------------|
| | L = 4 | S | L = 4 | S | L = 4 | S | |
| EBM Plasma Cathode | High cost, V = 4 | 16 | Width of lead brick High cost, V = 4 | 16 | Medium cost, V = 6 | 24 | 56 |
| UV-Mercury | Low cost, V = 8 | 32 | UV Sun glasses, Very cheap cost, V = 10 | 40 | Low cost V = 8 | 32 | 104 |
| UV-LED | Low cost, V = 8 | 32 | UV Sun glasses, Very cheap cost, V = 10 | 40 | Low cost V = 8 | 32 | 104 |

Table 8 Comparison of irradiator prototype technology for RVNRL in terms of time and difficulty of installation, operational costs and maintenance

| Type of irradiator | Installation time & difficulty | | Operational power (kW) | | Replacement of irradiators every year | | ΣS |
|--------------------|--------------------------------|----|---|----|---------------------------------------|----|------------|
| | L = 4 | S | L = 4 | S | L = 4 | S | |
| EBM Plasma Cathode | Long enough & difficult, V = 6 | 24 | (electron accelerator + equipment such as HV power supply, capacitor, vacuum system) = (5 + 18) = 23, V = 4 | 16 | There is no, V = 10 | 40 | 80 |
| UV-Mercury | Relatively fast & easy, V = 10 | 40 | UV-Mercury lamp (3) + 1 stirring motor (0.75) + feed pump (0.25) = 4, V = 10 | 40 | 3 times, V = 6 | 24 | 104 |
| UV-LED | Relatively fast & easy, V = 10 | 40 | UV-LED lamp (0.65) + 2 stirring motor (2 × 0.75) + water pump (0.5) + dose pump (0.5) = 3.15, V = 10 | 40 | There is no, V = 10 | 40 | 120 |

Table 9 Comparison of irradiator prototype technology for RVNRL in terms of HAZOP

| Type of irradiator | Dangerous level | | Radiation protection permit & audit | | Safety & security import irradiator | | ΣS |
|--------------------|--------------------------------------|----|---|----|-------------------------------------|----|------------|
| | L = 4 | S | L = 4 | S | L = 4 | S | |
| EBM Plasma Cathode | X-rays and ozon (medium level) V = 3 | 12 | Permits (construction, installation, operation) and periodic audits V = 4 | 16 | Quite difficult V = 5 | 20 | 48 |
| UV-Mercury | UVA radiation (Low level) V = 8 | 32 | Without permission V = 10 | 40 | Without security V = 10 | 40 | 112 |
| UV-LED | UVA radiation (Low level) V = 8 | 32 | Without permission V = 10 | 40 | Without security V = 10 | 40 | 112 |

From Table 6, 7, 8 and 9 we can determine the total value of the technology comparison (TC) for each type of irradiator for the RVNRL process as follows:

- Total value of TC of UV-LED irradiators = 140 + 104 + 120 + 112 = 476
- Total value of TC of UV-Mercury irradiators = 92 + 104 + 104 + 112 = 412

- Total value of TC of the plasma cathode-based EBM irradiators = 64 + 56 + 80 + 48 = 248.

Based on RVNRL technology comparison, UV-LED irradiators, UV-mercury irradiators, and the plasma cathode-based EBM irradiators give total value of 476, 412, and 248, respectively. Thus, it can be stated that the UV-LED irradiators technology for RVNRL is simpler, more practical, economical, and

environmentally friendly compared to the UV-mercury irradiators and EBM irradiators based on plasma cathodes.

4.0 CONCLUSION

The results of the technology comparison of the UV-LED irradiators, UV-mercury irradiators, and plasma cathode-based EBM irradiators for RVNRL are represented with a total value of 476, 412, and 248, respectively. Based on the results of the RVNRL technology comparison, it can be concluded that the UV-LED irradiators are simpler, more practical, economical, and environmentally friendly than the the UV-mercury irradiators and the plasma cathode-based EBM irradiators. Thus, it is worth considering using the irradiator prototype based on UV-LED lamp in small and medium businesses in the field of natural rubber latex agribusiness for RVNRL process.

Acknowledgement

This research is fully supported by a grant from the Ministry of Research, Technology and Higher Education of the Republic of Indonesia through the National Innovation System Research Incentive with the code RT-2015-0427. research can be carried out properly.

References

- [1] C. Widiyati and H. Poernomo. 2012. A Comparative Study of Early Pre-vulcanization Technology for Natural Rubber Latex with UV Radiation from the UV-mercury Lamp and from the Lamp of UV-Light Emitting Diode (UV-LED). *Proceedings of Meetings and Scientific Presentations on Accelerator Technology and Its Applications*. 14: 63-73. <http://digilib.batan.go.id/ppin/katalog/file/1411-1349-2012-063.pdf>.
- [2] H. Poernomo and R. Saptaji. 2012. Basic Design of Vulcanization of Natural Rubber Latex System with Electron Beam at Belt Conveyor. *Proceedings of the Meeting and Presentation of Basic Scientific-Research on Nuclear Science and Technology*. 14: 95-109. <http://digilib.batan.go.id/ppin/katalog/file/BP-18.pdf>.
- [3] N. A. Kinasih, M. I. Fathurrohman, and D. Suparto. 2015. Effect of Vulcanization Temperature on the Mechanical Properties of Vulcanized Natural and Acrylonitrile-Butadiene Rubbers. *Leather, Rubber and Plastics Magazines*. 31(2): 65-74. <http://ejournal.kemenperin.go.id/mkpp/article/view/504>.
- [4] F. E. Tambunan and H. Harahap. 2015. Effect of Vulcanization Temperature and Composition of Bentonite Clay Modified with Alkanolamide from RBDPKO Raw Material on Natural Rubber Latex Products. *Journal of Chemical Engineering*. 4(4): 64-70. <https://talenta.usu.ac.id/jtk/article/view/1515>.
- [5] R. Radford, H. Frain, M. P. Ryan, C. Slattery, and T. McMorrow. 2013. Mechanisms of Chemical Carcinogenesis in the Kidneys. *International Journal of Molecular Science*. 14: 19416-19433. Doi: 10.3390/ijms141019416.
- [6] Marsongko. 2013. Preparation of Gloves from Radiation Pre-vulcanized and Sulphur Vulcanized Natural Rubber Latex. *Packaging Chemistry Journal*. 35(2): 131-136. <http://ejournal.kemenperin.go.id/jkk/article/view/1885>.
- [7] J. Heathcote. 2010. UV-LED Overview Part I Operation and Measurement. Radtech Report. Technical Paper. 23-33. <https://www.radtech.org/magazinearchives/Publications/RadTechReport/jul-aug-2010/UV-LED%20Basics%20Part%20I-Operation%20and%20Measurement.pdf>.
- [8] Purepro. 2012. Ultraviolet Water Sterilizer. Pure-Pro Water Corp., Illinois, USA. <http://www.purepro.info/pdf/UV.pdf>.
- [9] P. Mill. 2012. UV Measurement for Formulators. EIT Instrument Markets. pmills@att.net.
- [10] J. Raymont. 2019. UV Measurement & Process Control: Theory vs. Reality Overview of EIT Products & Measurement Techniques, EIT Instrument Markets Sterling, Virginia USA. http://quimtech.com/archivos/Como_Medir_La_Radiaci%F3n_UV.pdf.
- [11] J. Raymont. 2001. Life After the Honeymoon: Getting to Know, Understand, Respect and Live with Your UV System and Process. *SGIA Journal*. Third Quarter: 29-39. https://www.eit.com/sites/default/files/resource-files/raymont_uv_system.pdf.
- [12] S. Schlögl, A. Temel, W. Kern, Leoben, R. Schaller, and A. Holzner. 2010. Manufacture of Non-Allergenic Surgical Gloves via UV Techniques. *Rohstoffe Und Anwendungen Raw Materials and Applications, KGK*. 187-191. https://www.kgk-rubberpoint.de/wp-content/uploads/migrated/paid_content/artikel/950.pdf.
- [13] S. Schlögl, N. Aust, R. Schaller, A. Holzner, and W. Kern. 2010. Survey of Chemical Residues and Biological Evaluation of Photochemically Pre-vulcanized Surgical Gloves. *Monatsh Chem*. 141: 1365-1372. <https://doi.org/10.1007/s00706-010-0404-3>.
- [14] S. Schlögl, A. Temel, R. Schaller, A. Holzner, and W. Kern. 2012. Characteristics of the Photochemical Pre-vulcanization in a Falling Film Photoreactor. *Journal of Applied Polymer*. 124: 3478-3486. <https://doi.org/10.1002/app.35457>.
- [15] S. Schlögl, M.L. Trutschel, W. Chassé, I. Letofsky-Papst, R. Schaller, A. Holzner, G. Riess, W. Kern, and K. Saalwächter. 2014. Photo-vulcanization Using Thiol-ene Chemistry: Film Formation, Morphology and Network Characteristics of UV Crosslinked Rubber Latices. *Polymer*. 55: 5584-5595. <https://doi.org/10.1016/j.polymer.2014.06.007>.
- [16] L. I. Mahmood. 2016. Preparation, Characterization and Applications of Biocomposites Consist of Chitosan Dispersed in Epoxidized Natural Rubber. Thesis submitted in fulfillment of the requirement for the degree of Doctor of Physosophy, University Sains Malaysia. http://eprints.usm.my/31355/1/LUQMAN_IDREES_MAHMO_OD_24.pdf.
- [17] J. Y. Zhang and I. W. Boyd. 2000. Lifetime Investigation of Excimer UV Sources. *Applied Surface Science*. 168: 296-299. [https://doi.org/10.1016/S0169-4332\(00\)00628-0](https://doi.org/10.1016/S0169-4332(00)00628-0).
- [18] K. Schindler, U. Leischner, P. Kaiser, T. Striebel, U. Schombs, and C. Lopper. 2017. High Intensity UV-LED Mask Aligner fo Applications in Industrial Research. SUSS Report. <https://ieeexplore.ieee.org/abstract/document/8278704>.
- [19] K. Holz, J. Lietard, M. M. Somoza. 2017. High-Power 365 nm UV LED Mercury Arc Lamp Replacement for Photochemistry and Chemical Photolithography. *ACS Sustainable Chem. Eng.* 5: 828-834. <https://doi.org/10.1021/acssuschemeng.6b02175>.
- [20] C. Widiyati and H. Poernomo. 2018. Design of a Prototype Photoreactor UV-LEDs for Radiation Vulcanization of Natural Rubber Latex. *International Journal of Technology*. 1: 130-141. <https://doi.org/10.14716/ijtech.v9i1.1164>.
- [21] P. Raharjo, K. Uemura, N.N. Koval, V. Shugurov, V. Denisov, V. Jakovlev, W. Setiawan, and M. Utama. 2008. Application of Large Area Plasma Cathode Electron Beam for Natural Rubber Vulcanization. *Proceedings of 15th International Symposium on High Current Electronics*.

- 497-501.
https://www.researchgate.net/publication/237794855_Application_of_Large_Area_Plasma_Cathode_Electron_Beam_for_Natural_Rubber_Vulcanization.
- [22] S. S. Kovalskiy. 2017. Low-Energy Electron Beam for Medical and Plasma Chemistry Applications. Beam & Plasma Technologies. LLC, Tomsk, Rusia.
- [23] C. Widiyati and H. Poernomo, 2015. Photoreactor Design Concept Based on Irradiator UV-LED for Pre-Vulcanise Natural Rubber Latex. *Proceedings of National Seminar of Nuclear Energy Technology*. 1: 543-555. <http://www.batan.go.id/images/Seminar/SENTEN2016/SENTEN-26april-2016-v2.pdf>.
- [24] S. A. Korenev and R.P. Johnson. 2007. Pulsed Low Energy Electron Sources for Material Surface Modification. *Pulsed Power Conference, 2007 16th IEEE International*. 65-68. http://www.muonsinternal.com/muons3/tiki-download_wiki_attachment.php?attId=179.
- [25] IAEA. 2003. Use of Mathematical Modelling in Electron Beam Processing: A Guidebook. IAEA Radiation Technology Series No. 1. 55-57, 78. https://www-pub.iaea.org/MTCD/publications/PDF/Pub1474_Web.pdf.
- [26] Z. Zimek. 1998. Electron Accelerators for Environment Protection, Institute of Nuclear Chemistry and Technology, Warsaw, Poland. <https://inis.iaea.org/collection/NCLCollectionStore/Public/31/003/31003497.pdf>.
- [27] International Irradiation Association. 2011. Industrial Radiation with Electron Beams and X-rays. http://iiaglobal.com/uploads/documents/Industrial_Radiation_eBeam_Xray.pdf.
- [28] Z. Zimek, 2017. Comparison between EB, Gamma, and X-Rays Facilities for Radiation Processing. Centre for Radiation Research and Technology, Institute of Nuclear Chemistry and Technology, Warsaw, Poland. <https://ec.europa.eu/programmes/erasmus-plus/project-result-content/cc85291e-3a92-4ae1-b358-0ad68cbff1c0/L3-Comparison-Zimek.pdf>.
- [29] Patent 7026749. Cathode for Electron Tube and Method of Preparing the Same. <https://patents.google.com/patent/US7026749B2/en>.
- [30] C. E. Harries. 2000. Survey of Breakthrough Materials. The Center of Excellence for Structures and Materials, NASA Langley Research Center. Materials Survey. 1-86. https://history.nasa.gov/DPT/Technology%20Priorities%20Recommendations/Breakthrough%20Materials%20DPT%20Jul_00.pdf.
- [31] D. Q. Kern. 1983. *Process Heat Transfer*. Mc. Graw Hill International Book Company. 805. https://sv.20file.org/up1/423_0.pdf.
- [32] H. Handayani, A. Cifriadi, S. Puspitasari, A. Ramadhani, Darsono, E. Nuraini. 2019. The Influence of Latex Vulcanization with Irradiation using Electron Beams Machine on Latex Goods Mechanical Properties and Protein Content. *Indonesian J. Nat. Rubb. Res.* 37 (2): 207-216. <https://doi.org/10.22302/ppk.jpk.v3i2.661>.
- [33] E. Nuraini, Darsono, W. Andriyanti, Saefurrochman, Sutadi, S.R. Adabiah. 2021. The Effect of Stirring Speed Variations on the Mechanical Properties of Latex Post-irradiation Using the ARJUNA 1.0 Electron Beam. AIP Conference Proceedings. 2381: 020050. <https://doi.org/10.1063/5.0067329>.
- [34] M. Reowdecha, P. Dittanet, P. Sae-oui, S. Loykulnant, P. Prapainainar. 2021. Film and Latex Forms of Silica-reinforced Natural Rubber Composite Vulcanized Using Electron Beam Irradiation. *Heliyon*. 7(2021): e07176. <https://doi.org/10.1016/j.heliyon.2021.e07176>.
- [35] R. Hidayat. 2011. Guidelines for Reviewing Papers for Seminars and Scientific Journals. Post-Graduate in Electrical Engineering, Faculty of Engineering, Gadjah Mada University, <http://te.ugm.ac.id/~risanuri/v01/wp-content/uploads/2011/02/bagaimana-review-paper.pdf>.